Biochemistry and Biophysics Reports 27 (2021) 101046

Contents lists available at ScienceDirect

Biochemistry and Biophysics Reports

journal homepage: www.elsevier.com/locate/bbrep

# Interleukin-1β enhances cell adhesion in human endothelial cells via microRNA-1914–5p suppression

Toshie Kihara [a,1], Kohki Toriuchi [a,1], Hiromasa Aoki [a], Hiroki Kakita [a,b], Yasumasa Yamada [b], Mineyoshi Aoyama [a,*]

[a] Department of Pathobiology, Nagoya City University Graduate School of Pharmaceutical Sciences, 3-1 Tanabe-dori, Mizoho-ku, Nagoya, Aichi, 467-8603, Japan
[b] Department of Perinatal and Neonatal Medicine, Aichi Medical University, 1-1 Yazakokarimata, Nagakute, Aichi, 480-1195, Japan

ARTICLE INFO

*Keywords:*
Atherosclerosis
IL-1β
miR-1914–5p
Endothelial cells
Monocyte adhesion

ABSTRACT

Atherosclerosis is a chronic inflammatory disease and the underlying cause of most cardiovascular diseases. Interleukin (IL)-1β facilitates early atherogenic lesion formation by increasing monocyte adhesion to endothelial cells via upregulation of adhesion molecules, including intercellular adhesion molecule-1 (ICAM-1). MicroRNAs (miRNAs) have been shown to be associated with inflammatory conditions in the vascular system. The expression of circulating miR-1914–5p is reportedly downregulated in patients with cardiovascular diseases. However, the role of miR-1914–5p downregulation in IL-1β–induced endothelial cell dysfunction and the effect of miR-1914–5p on lesion formation remain unclear. Therefore, we investigated whether miR-1914–5p is associated with monocyte adhesion in human endothelial cells. IL-1β decreased miR-1914–5p expression in EA.hy926 cells. In addition, miR-1914–5p depletion enhanced ICAM-1 expression and monocyte adhesion in EA.hy926 cells. Moreover, miR-1914–5p mimic suppressed monocyte adhesion and ICAM-1 expression induced by IL-1β in endothelial cells. These results suggest that suppression of miR-1914–5p expression by IL-1β may be an important regulator in mediating monocyte adhesion in endothelial cells. Further investigation of miR-1914–5p may lead to the development of novel therapeutic strategies for atherosclerosis.

## 1. Introduction

Atherosclerosis is a chronic inflammatory disease and the underlying cause of most cardiovascular diseases [1,2]. The atherogenic process is triggered by focal endothelial activation and adhesion of monocytes [3]. Following adhesion to the endothelium, monocytes migrate into the subendothelial layer of the intima in response to chemotactic factors such as chemokines [4]. Invading monocytes differentiate into macrophages in response to cytokine and/or growth factor stimulation in the inflamed intima, and these macrophages engulf lipoproteins via scavenger receptors, which leads to the formation of plaque [5].

Pro-inflammatory cytokines promote the process of lesion formation and susceptibility to plaque development [1]. Interleukin (IL)-1β, the prototypical inflammatory cytokine, is produced by several cell types in response to various stimuli and functions as a critical early mediator of inflammation [6,7]. IL-1β facilitates early atherogenic lesion formation by increasing monocyte adhesion to endothelial cells via upregulation of the expression of adhesion molecules, including intercellular adhesion molecule-1 (ICAM-1) [8–10]. Indeed, the results of recent phase clinical 3 trials indicated that suppression of IL-1β signaling via the monoclonal antibody canakinumab markedly reduces the risk of major adverse cardiovascular events, highlighting the important role of IL-1β in cardiovascular disease [11,12]. Identification of novel mechanisms to mitigate the effects of IL-1β on atherogenesis may therefore be important in the search for new therapeutic candidates [12].

MicroRNAs (miRNAs) are defined as short, single-stranded, non-coding RNA molecules that regulate the synthesis of proteins through messenger RNA (mRNA) degradation or translational repression [13,14]. It has been suggested that miRNAs control the inflammatory state of the vasculature by affecting the activation and infiltration of leukocytes via the vascular wall [15,16]. The miRNA miR-126–3p was shown to affect both vascular dysfunction and inflammation [17,18]. We

* Corresponding author. Department of Pathobiology Nagoya City University, Graduate School of Pharmaceutical Sciences, 3-1, Tanabe-dori, Mizuho-ku, Nagoya, 467-8603, Japan.
*E-mail addresses:* toshie6776@gmail.com (T. Kihara), taka1212oka@yahoo.co.jp (K. Toriuchi), haoki@phar.nagoya-cu.ac.jp (H. Aoki), haoki@phar.nagoya-cu.ac.jp (H. Kakita), yamasan@aichi-med-u.ac.jp (Y. Yamada).
[1] These authors contributed equally to this work.

https://doi.org/10.1016/j.bbrep.2021.101046
Received 20 April 2021; Received in revised form 28 May 2021; Accepted 6 June 2021

previously reported that IL-6 promotes monocyte adhesion in human endothelial cells via miR-126–3p suppression [19]. Thus, understanding the effect of miRNAs on the progression of arteriosclerosis, their role in the process of vascular disease development, and their potential uses in clinical therapy could be important [13]. Recently, another research group demonstrated that expression of circulating miR-1914–5p was downregulated in patients with cardiovascular diseases [20]. However, the role of miR-1914–5p downregulation in inflammatory cytokine–induced endothelial cell dysfunction and the effect of miR-1914–5p on lesion formation remain unclear.

In the present study, we examined the effects of IL-1β on endothelial cell responses by miR-1914–5p inhibition in human endothelial cells. We also investigated whether exogenous miR-1914–5p decreased IL-1β–induced monocyte adhesion.

## 2. Materials and methods

### 2.1. Culture of EA.hy926 and THP-1 cells

EA.hy926 human vascular endothelial cells and THP-1 human monocytes were purchased from the American Type Culture Collection (Manassas, VA, USA). Cells were cultured at 37 °C in a 5% $CO_2$/95% air environment and sub-cultured every third or fourth day. EA.hy926 cells were grown in high-glucose (4500 mg/L) Dulbecco's Modified Eagle's Medium (Wako, Osaka, Japan) supplemented with 10% fetal bovine serum (FBS), 100 U/mL penicillin, and 100 μg/mL streptomycin. For IL-1β treatment experiments, EA.hy926 cells were re-plated on 60-mm tissue culture dishes at $3 \times 10^5$ cells/dish. After the culture medium was replaced with fresh FBS-free medium, IL-1β (Wako) was added to the medium at the indicated concentration. We chose to use the maximum concentration of IL-1β (10 ng/mL) for stimulation because most previous studies have used this concentration. THP-1 cells were grown in RPMI-1640 (Wako) medium supplemented with 10% FBS, 100 U/mL penicillin, and 100 μg/mL streptomycin.

### 2.2. Transfection

Hsa-miR-1914–5p inhibitor (MISSION® Synthetic miRNA Inhibitor Human hsa-miR-1914–5p) and mimic (MISSION® Synthetic miRNA mimic Human hsa-miR-1914–5p) were purchased from Sigma (St. Louis, MO, USA). As controls, inhibitor-NC (MISSION® Synthetic miRNA Inhibitor Negative Control 1, Sigma) or mimic-NC (MISSION® Synthetic miRNA mimic Negative Control 1, Sigma) were used. Transient transfections were performed using Lipofectamine RNAi Max (Invitrogen, Carlsbad, CA, USA), according to the manufacturer's instructions. EA.hy926 endothelial cells were transfected with miR-1914–5p inhibitor or mimic at a final concentration of 10 nM for 24 h, according to the manufacturer's recommended concentration and incubation time. Inhibitor-NC– or mimic-NC–transfected cells exhibited no significant difference compared with the non-transfected control group.

### 2.3. miRNA isolation and quantitative reverse transcription–polymerase chain reaction (qRT-PCR)

Small RNAs (<200 bp) were isolated using ISOGEN II (Nippon Gene, Toyama, Japan), according to the manufacturer's instructions. miRNA reverse transcription (RT) was performed using the TaqMan microRNA Reverse Transcription kit (Thermo Fisher Scientific, San Diego, CA, USA). Reaction tubes were kept on ice for at least 5 min, followed by incubation in a thermal cycler at 16 °C for 30 min, 42 °C for 30 min, and 85 °C for 5 min. Subsequently, quantitative real-time PCR was performed in a PCR reaction solution containing 2 μL RT product, 0.5 μL 20 × TaqMan Micro RNA Assay containing PCR primers and probes, 5 μL 2 × TaqMan Universal PCR Master Mix Probe Master (Roche, Ltd., Basel, Switzerland), and 2.5 μL nuclease-free $H_2O$. Primer pairs and TaqMan probes were purchased from Thermo Fisher Scientific. The reaction mix was first incubated at 50 °C for 2 min and then 95 °C for 10 min, followed by 50 cycles at 95 °C for 15 s and 60 °C for 1 min. Reactions were performed using the Thermal Cycler Dice Real-Time System (Takara Bio, Inc., Otsu, Japan). Expression of each miRNA was normalized to the expression of miR-16 as a housekeeping miRNA.

### 2.4. Target gene prediction

Target mRNAs with potential binding sites for miR-1914–5p were identified by searching against miRDB database (http://mirdb.org), a public database [21,22]. Predicted genes were selected based on high prediction scores in relationship to roles in hypertension, diabetes mellitus, cardiac disease, and/or endothelial cell function.

### 2.5. qRT-PCR

qRT-PCR was performed on selected genes using the Thermal Cycler Dice Real-Time System (Takara Bio, Inc.). Total RNA was extracted from samples using RNAiso plus (Takara Bio, Inc.) with phenol-chloroform, and cDNAs were generated using PrimeScript RT Master Mix (Takara Bio, Inc.). Real-time PCR was performed using Go Taq (Promega Corp., Madison, WI, USA). Each reaction was performed in a total volume of 12.5 μL containing 2.5 μL RT product, 0.5 μL forward primer (10 μM), 0.5 μL reverse primer (10 μM), 6.25 μL Go Taq qPCR Master Mix, and 2.75 μL nuclease-free $H_2O$. Amplification was performed at 95 °C for 2 min, followed by amplification for 40 cycles at 95 °C for 15 s and 55 °C for 1 min. We normalized the relative target gene transcript levels to endogenous transcript levels of a housekeeping gene (the *ACTB* locus), after confirming that the cDNAs from different genes were amplified with the same efficiency. The primer pairs used for amplification are shown in Table 1.

### 2.6. Cell adhesion assay

Monocyte adhesion was assayed as previously described [19]. EA.hy926 cells seeded in 35-mm glass-bottom culture dishes (Matsunami Glass, Inc., Ltd., Osaka, Japan) at $3 \times 10^5$ cells/dish were stimulated with IL-1β or transfected with miRNA inhibitor/mimic. THP-1 monocytes were washed with serum-free RPMI 1640 medium and suspended at $1 \times 10^6$ cells/mL in medium with 10 μM BCECF-AM (Dojindo Laboratories, Kumamoto, Japan) and kept at 37 °C for 1 h. Stimulated EA.hy926 cells were washed once with serum-free RPMI 1640, and $3 \times 10^5$ BCECF-AM–loaded THP-1 cells were added to each well. After 1 h of incubation, the adherent cells were gently washed three times with RPMI 1640, and non-adherent cells were washed out. Fluorescent images were obtained using an LSM800 confocal microscope (Carl Zeiss, Germany). The number of THP-1 cells per view was also quantified from randomly acquired images.

**Table 1**
Primer pairs used for polymerase chain reaction amplification.

| Gene | Primer sequences |
|---|---|
| ***ACTB*** | **Forward: GATCAAGATCATTGCTCCTCCT** |
| | **Reverse: GGGTGTAACGCAACTAAGTCA** |
| ***ICAM-1*** | **Forward: CAACCTCAGCCTCGCTATGG** |
| | **Reverse: CGGGGCAGGATGACTTTTGA** |
| ***ACADSB*** | **Forward: TGGAATACACTTTGCTCCCCT** |
| | **Reverse: CCATGGTTGAAACCAAAGGTG** |
| ***RBMS1*** | **Forward: GTACCCTCAGTACGCCACCT** |
| | **Reverse: GTGGGCTGGGACCAGAGA** |
| ***ZBTB10*** | **Forward: TGGTGCCAAAAGACCCCTG** |
| | **Reverse: GTCACAGTACCCCTCCTCTG** |

Sequences of primer pairs for *ACTB* (actin-beta), *ICAM-1* (intercellular adhesion molecule-1), *ACADSB* (acyl-CoA dehydrogenase short/branched chain), *RBMS1* (RNA binding motif single-stranded interacting protein 1), and *ZBTB10* (zinc finger and BTB domain containing 10).

### 2.7. Immunocytochemistry

EA.hy926 endothelial cells were grown on glass coverslips in a 24-well plate ($1.0 \times 10^5$ cells/well) coated with BD Matrigel Basement Membrane Matrix Growth Factor Reduced (BD Bioscience, San Jose, CA, USA). Attached cells were washed with phosphate-buffered saline (PBS) and then fixed with 3% paraformaldehyde in PBS for 30 min. After three washes with PBS, the cells were incubated with 3% bovine serum albumin and 0.1% glycine in PBS for 1 h to block non-specific binding. Cells then were incubated overnight at 4 °C with the primary antibody, anti–ICAM-1 (also known as CD54; rabbit polyclonal; 1:400; R&D Systems, Minneapolis, MN, USA). After three washes with PBS, the cells were incubated with Alexa Fluor 594–conjugated secondary antibody (1:1000; Invitrogen) for 1 h in the dark. Finally, coverslips were mounted onto glass slides with ProLong Diamond antifade reagent containing 4′,6′diamidino2phenylindole (DAPI; Invitrogen). An LSM800 confocal microscope (Carl Zeiss) was used to visualize stained cells. Mean staining intensity was determined using ImageJ software (National Institutes of Health, Bethesda, MD, USA).

### 2.8. Statistical analysis

All statistical analyses were performed using EZR (Saitama Medical Center, Jichi Medical University, Saitama, Japan), which is a graphical user interface for R (The R Foundation for Statistical Computing, Vienna, Austria). More precisely, EZR is a modified version of R Commander designed to add statistical functions frequently used in biostatistics [23]. Comparisons of continuous data between three or more groups were performed using two-tailed analysis of variance (ANOVA) with post hoc Bonferroni test. Comparisons between data from two groups were performed using two-tailed non-paired Student's *t*-tests. Data are reported as the mean ± standard error of the mean (SEM). Statistical significance was set at $p < 0.05$.

## 3. Results

### 3.1. Expression of miR-1914–5p was downregulated by exposure to IL-1β in human endothelial cells

To examine the relationship between IL-1β and miR-1914–5p expression, we performed a quantitative analysis of miR-1914–5p levels. Accumulation of miR-1914–5p was attenuated by IL-1β in EA.hy926 human endothelial cells (Fig. 1A). We also analyzed the expression of miR-126–3p, which we previously showed is associated with the regulation of cell adhesion by IL-6 [19]. IL-1β exposure had no significant effect on miR-126–3p expression in EA.hy926 cells (Fig. 1B).

### 3.2. Adhesion of human monocytes to human endothelial cells was enhanced by IL-1β exposure

Recruitment of circulating monocytes from the bloodstream and adhesion to the endothelium are hypothesized as playing roles in the early stage of atherosclerotic plaque formation [24]. Therefore, we performed a cell adhesion assay and assessed adhesion of THP-1 human monocytes to IL-1β–exposed EA.hy926 cells. Adhesion of THP-1 cells to IL-1β–exposed EA.hy926 cells was enhanced compared to cells incubated in the absence of IL-1β (Fig. 2A and B).

### 3.3. ICAM-1 expression was upregulated by IL-1β treatment in human endothelial cells

ICAM-1 is expressed on the surface of endothelial cells and plays a key role in monocyte adhesion [25]. Therefore, ICAM-1 levels were determined by quantitative RT-PCR and immunocytochemistry in EA.hy926 cells. IL-1β exposure increased the accumulation of transcripts of the *ICAM-1* gene (Fig. 2C). Additionally, higher-intensity ICAM-1 immunostaining demonstrated that expression of ICAM-1 protein in EA.hy926 cells was upregulated in the presence of IL-1β (Fig. 2D). Using ImageJ software, we quantified the mean immunostaining intensity and confirmed a statistically significant difference (Fig. 2E).

### 3.4. Inhibition of miR-1914–5p expression enhanced adhesion of human monocytes to human endothelial cells

We next examined whether inhibition of miR-1914–5p expression in EA.hy926 cells affects the adhesion of monocytes to endothelial cells. First, we confirmed that miR-1914–5p accumulation in EA.hy926 cells was suppressed by a miRNA inhibitor of human miR-1914–5p (Fig. 3A). We also confirmed that the miR-1914–5p inhibitor increased the expression of target genes as well as IL-1β (Fig. S1A and S1B). Furthermore, EA.hy926 cells in which miR-1914–5p expression was suppressed exhibited increased adherence of THP-1 cells even in the absence of IL-1β (Fig. 3B and C). EA.hy926 cells in which miR-1914–5p expression was low exhibited increased *ICAM-1* gene expression and mean ICAM-1 immunostaining intensity (Fig. 3D, E, F).

### 3.5. Overexpression of miR-1914–5p suppressed adhesion of human monocytes to IL-1β–exposed human endothelial cells

We also examined whether exogenous miR-1914–5p suppressed the adhesion of THP-1 cells to EA.hy926 cells. Initial experiments confirmed an increase in miR-1914–5p accumulation in EA.hy926 cells treated with a human miR-1914–5p miRNA mimic (Fig. 4A). We also confirmed that the miR-1914–5p miRNA mimic reduced the expression of target genes (Fig. S1C). EA.hy926 cells that overexpressed miR-1914–5p

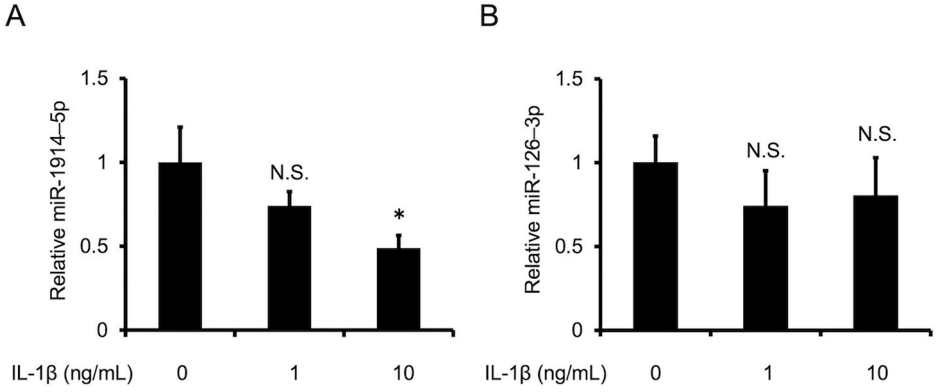


**Fig. 1.** IL-1β exposure decreased miR-1914–5p expression. EA.hy926 cells were incubated with IL-1β for 24 h, and miRNA expression was examined by real-time RT-PCR. Relative expression of (A) miR-1914–5p and (B) miR-126–3p. Data are mean ± SEM (n = 3 in each group). *$p < 0.05$ compared with the vehicle group.

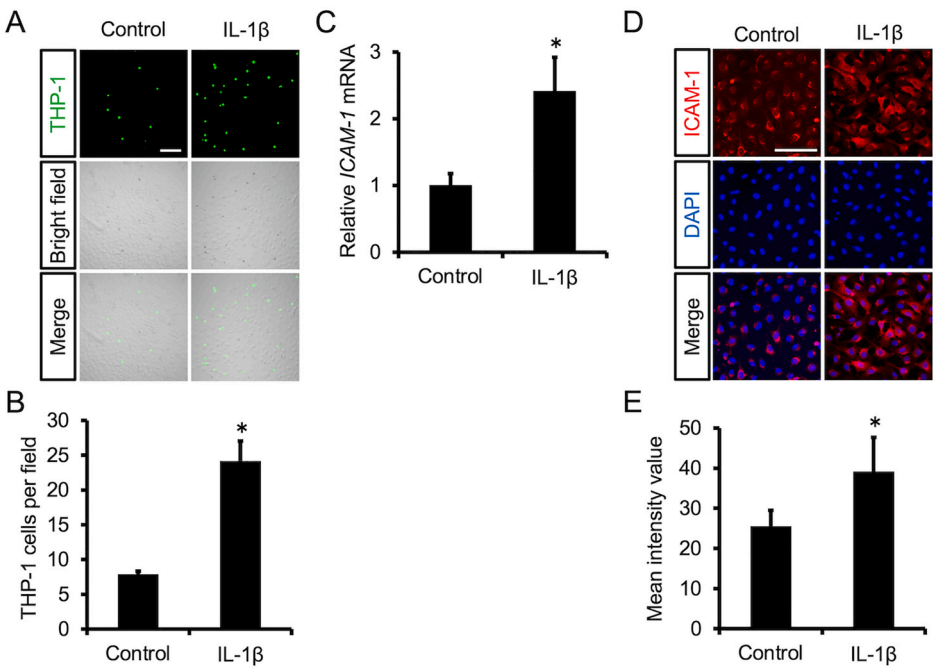


**Fig. 2.** Effects of IL-1β on monocyte adhesion to human endothelial cells. (A) Adhesion of THP-1 cells to a monolayer of EA.hy926 cells following 1 h co-culture after IL-1β (10 ng/mL) treatment of EA.hy926 cells for 24 h. Scale bar represents 100 μm. (B) Number of fluorescent THP-1 monocytes on the EA.hy926 cell monolayer. Data are mean ± SEM (n = 6 fields in each group). *$p < 0.05$ compared with the control group. (C) EA.hy926 cells were incubated with IL-1β (10 ng/mL) for 24 h, and *intercellular adhesion molecule-1* (*ICAM-1*) gene expression was examined by real-time RT-PCR. Data are mean ± SEM (n = 3 in each group). *$p < 0.05$ compared with the control group. (D) Immunocytochemical detection of ICAM-1 in human endothelial cells treated with IL-1β. ICAM-1 protein expression was assessed in EA.hy926 cells cultured as a monolayer and treated with IL-1β (10 ng/mL) for 24 h. Staining with anti–ICAM-1 antibody (red). Nuclei were stained with DAPI (blue). Scale bar represents 100 μm. (E) Semi-quantitative analysis of ICAM-1 protein as determined using ImageJ software. Data are mean ± SEM (n = 6 fields in each group). *$p < 0.05$ compared with the control group. (For interpretation of the references to color in this figure legend, the reader is referred to the Web version of this article.)

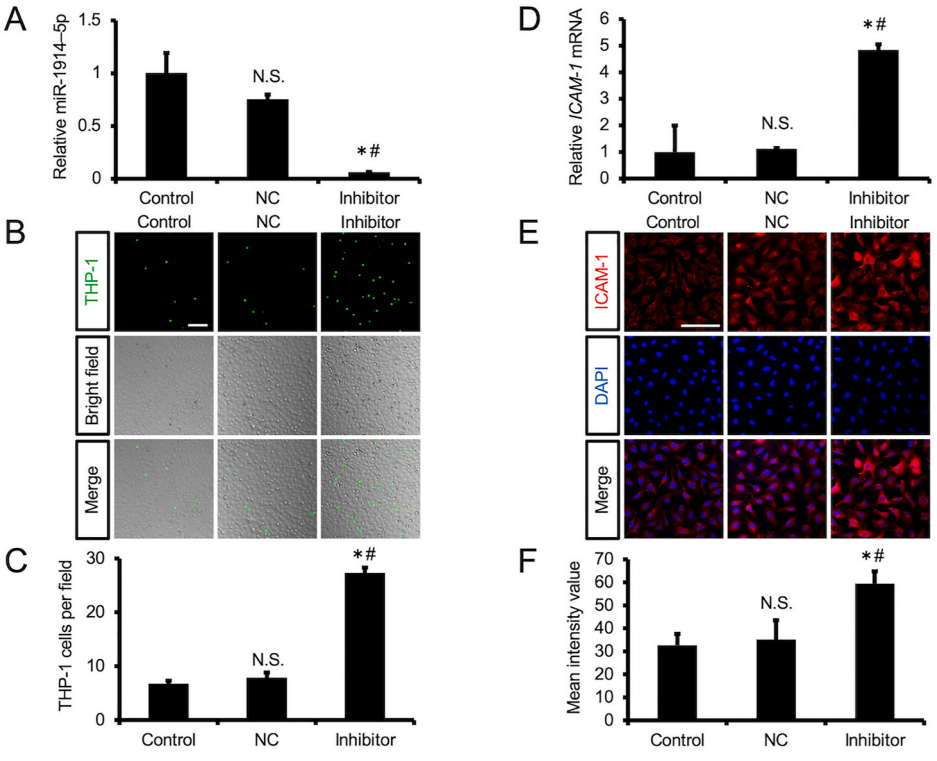


**Fig. 3.** Transfection of miR-1914–5p inhibitor increased monocyte adhesion and ICAM-1 expression in human endothelial cells. (A) EA.hy926 cells were transfected with miR-1914–5p inhibitor or negative control (NC) inhibitor for 24 h miR-1914–5p levels were then assessed by real-time RT-PCR. The miR-1914–5p inhibitor significantly suppressed miR-1914–5p accumulation in EA.hy926 cells compared with the control and NC. Data are mean ± SEM (n = 3 per group). *$p < 0.05$ compared with the control. #$p < 0.05$ compared with the *NC*-transfected group. (B) EA.hy926 cells were transfected with miR-1914–5p inhibitor or NC for 24 h. Adhesion of THP-1 cells to the EA.hy926 cell monolayer following 1 h of co-culture after transfection of EA.hy926 cells with miR-1914–5p inhibitor for 24 h. Scale bar represents 100 μm. (C) Number of fluorescent THP-1 monocytes on the EA.hy926 cell monolayer. Data are mean ± SEM (n = 6 fields in each group). *$p < 0.05$ compared with the control group. #$p < 0.05$ compared with the *NC*-transfected group. (D) EA.hy926 cells were transfected with miR-1914–5p inhibitor or NC for 24 h, and *ICAM-1* gene expression was examined by real-time RT-PCR. Data are mean ± SEM (n = 3 in each group). *$p < 0.05$ compared with the control group. #$p < 0.05$ compared with the *NC*-transfected group. (E) Effect of miR-1914–5p inhibitor on ICAM-1 protein expression in human endothelial cells. EA.hy926 cells were transfected with miR-1914–5p inhibitor or NC for 24 h. ICAM-1 expression was examined in EA.hy926 cells by immunocytochemical analysis. Staining with anti–ICAM-1 antibody (red). Nuclei were stained with DAPI (blue). Scale bar represents 100 μm. (F) Semi-quantitative analysis of ICAM-1 protein as determined using ImageJ software. Data are mean ± SEM (n = 6 fields in each group). *$p < 0.05$ compared with the control group. #$p < 0.05$ compared with the *NC*-transfected group. (For interpretation of the references to color in this figure legend, the reader is referred to the Web version of this article.)

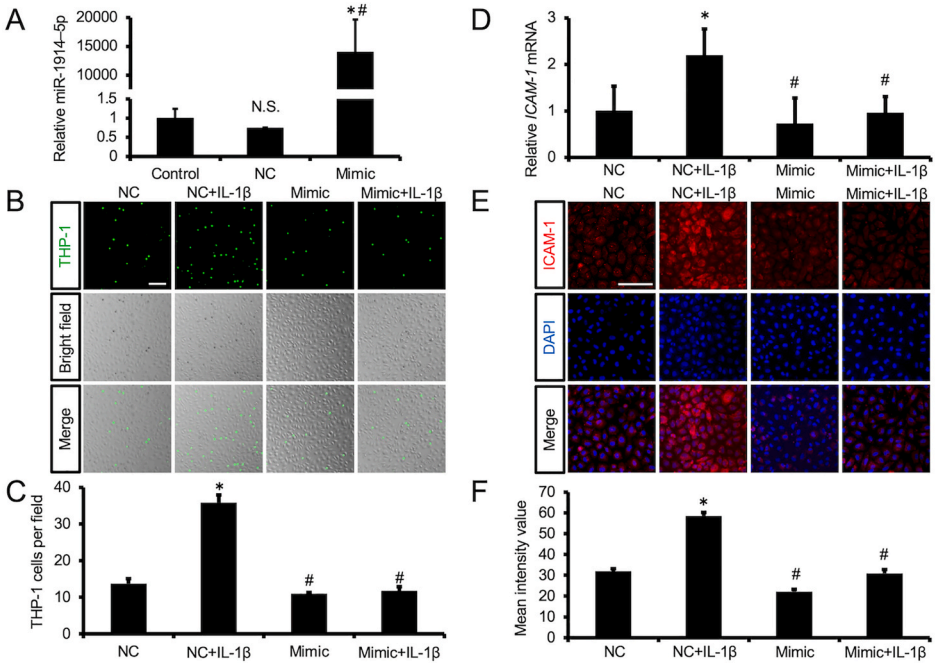


**Fig. 4.** Transfection of miR-1914–5p mimic suppressed IL-1β–induced monocyte adhesion and IL-1β–induced ICAM-1 expression in human endothelial cells. (A) EA.hy926 cells were transfected with miR-1914–5p mimic or negative control (NC) mimic for 24 h miR-1914–5p levels then were assessed by real-time RT-PCR. The miR-1914–5p mimic significantly increased miR-1914–5p expression in EA.hy926 cells compared with the control and NC. Data are mean ± SEM (n = 3 per group). $^{*}p < 0.05$ compared with the control. $^{\#}p < 0.05$ compared with the *NC*-transfected group. (B) EA.hy926 cells were transfected with miR-1914–5p mimic or NC for 24 h. EA.hy926 cells were incubated with IL-1β for 24 h after the 24-h transfection. After 24 h of IL-1β treatment, adhesion of THP-1 cells to the EA.hy926 cell monolayer was assessed following 1 h of co-culture. Scale bar represents 100 μm. (C) Number of fluorescent THP-1 monocytes on the EA.hy926 cell monolayer. Data are mean ± SEM (n = 6 fields in each group). $^{*}p < 0.05$ compared with the NC group. $^{\#}p < 0.05$ compared with the NC + IL-1β group. (D) EA.hy926 cells were incubated with IL-1β for 24 h after the 24-h transfection with miR-1914–5p, and *ICAM-1* gene expression was examined by real-time RT-PCR. Data are mean ± SEM (n = 3 in each group). $^{*}p < 0.05$ compared with the NC group. $^{\#}p < 0.05$ compared with the NC + IL-1β group. (E) Effect of miR-1914–5p mimic on ICAM-1 protein expression in human endothelial cells. EA.hy926 cells were transfected with miR-1914–5p mimic or NC for 24 h. EA.hy926 cells were incubated with IL-1β for 24 h after the 24-h transfection. After 24 h of IL-1β treatment, ICAM-1 expression was examined in EA.hy926 cells by immunocytochemical analysis. Staining with anti–ICAM-1 antibody (red). Nuclei were stained with DAPI (blue). Scale bar represents 100 μm. (F) Semi-quantitative analysis of ICAM-1 protein as determined using ImageJ software. Data are mean ± SEM (n = 6 fields in each group). $^{*}p < 0.05$ compared with the NC group. $^{\#}p < 0.05$ compared with the NC + IL-1β group. (For interpretation of the references to color in this figure legend, the reader is referred to the Web version of this article.)

exhibited decreased adhesion of THP-1 cells even in the presence of IL-1β (Fig. 4B and C). Furthermore, miR-1914–5p overexpression reduced *ICAM-1* gene expression and IL-1β–induced enhancement of ICAM-1 immunoreactivity to the same degree as the negative control group (Fig. 4D, E, F).

## 4. Discussion

In the present study, we evaluated whether IL-1β affects the expression of miR-1914–5p in EA.hy926 human endothelial cells. IL-1β decreased miR-1914–5p expression in EA.hy926 cells (Fig. 1). These results are consistent with reported higher IL-1β levels and lower miR-1914–5p expression in patients with coronary artery disease [6,20,26]. IL-1β is also associated with diabetes mellitus, which is closely related to atherosclerosis [12,27]. Therefore, the relationship between IL-1β and miR-1914–5p should be evaluated in patients with more diverse backgrounds. The RNA binding motif single-stranded interacting protein 1 (RBMS1) gene, which is a target of miR-1914–5p, is reportedly associated with diabetes [28]. Several target genes, including RBMS1, exhibited expected changes upon IL-1β stimulation or manipulation of miR-1914–5p expression in the present study (Fig. S1) [29,30]. These results suggest that miR-1914–5p plays a complex role in regulating the physiology and pathology of atherosclerosis.

There is growing evidence that miRNAs are involved in the pathology of atherosclerosis, including endothelial cell dysfunction [31]. Our present data demonstrate that miR-1914–5p degradation enhances ICAM-1 expression and monocyte adhesion to endothelial cells (Figs. 2 and 3). Treatment with a miR-1914–5p mimic was found to suppress monocyte adhesion and ICAM-1 expression induced by IL-1β in endothelial cells (Figs. 2 and 4). Binding of IL-1β to its receptor initiates a signaling cascade that promotes ICAM-1 expression via activation of NF-κB, a master regulator of inflammatory gene expression [32,33]. Tripartite motif containing 14 (TRIM14), a target gene of miR-1914–5p, is reportedly involved in the expression of ICAM-1 and VCAM-1 (vascular cell adhesion molecule-1) in endothelial cells via activation of NF-κB [34]. However, TRIM14 expression was not reproducible in the present study, and thus the effect could not be confirmed (data not shown). TNFα, a representative pro-inflammatory cytokine along with IL-1β, promotes increased expression of adhesion molecules such as VCAM-1 by downregulating the expression of miR-181b [35]. In the proposed mechanism, miR-181b inhibits the nuclear translocation of NF-κB by decreasing the expression of importin-3α (a member of a family of proteins involved in nuclear translocation) [35]. Regulation of ICAM-1 expression by miR-1914–5p may also involve the modulation of inflammatory signaling, including nuclear transfer of the NF-κB complex.

Activation of NF-κB induced by IL-1β leads to oxidative stress and further cytokine production, which in turn may lead to further endothelial damage and expression of adhesion factors [8,36]. We showed that the expression of at least ICAM-1 is regulated by miR-1914–5p in the presence of IL-1β. Examining direct interactions between miR-1914–5p and other cytokines or oxidative stress could be a key to clarifying the role of miR-1914–5p in the presence of IL-1β [33,37]. Although VCAM-1 and ICAM-1 are similar adhesion factors, persistent expression of ICAM-1 is reportedly induced by IL-1β, whereas VCAM-1 expression is only transiently induced [38]. Therefore, it is likely that ICAM-1 plays an important role in the more continuous increase in monocyte adhesion observed during IL-1β or miR-1914–5p inhibitor stimulation. However, it is possible that the expression of other adhesion factors, including VCAM-1, is also altered at an earlier stage. In addition to the adhesion molecules, it will be important to comprehensively analyze factors induced by IL-1β, such as cyclooxygenase-2 and

inducible nitric oxide synthase [39].

In this study, we used an *in vitro* experimental model to confirm the direct relationship between miR-1914–5p and monocyte adhesion induced by IL-1β in endothelial cells. However, because miRNAs are intricately regulated *in vivo*, the limitations of cellular experiments must be taken into account. Investigations using an animal model of atherosclerosis will be necessary to evaluate the function of miR-1914–5p in the context of variable expression of other miRNAs [20]. It will also be critical to clarify the role of miR-1914–5p in cells other than vascular endothelial cells in order to develop therapeutic strategies. miR-1914–5p expression is reportedly increased in biopsy samples of colorectal cancer tissue [40]. The effects of miR-1914–5p on other tissues and cells should be evaluated in combination with *in vivo* and *in vitro* experiments. Drug dosage, duration of administration, and delivery issues also need to be addressed.

In conclusion, we identified miR-1914–5p as an IL-1β–responsive miRNA that suppresses ICAM-1 expression and adhesion of THP-1 human monocytes to EA.hy926 human endothelial cells. Furthermore, exogenous miR-1914–5p counteracted the enhancement of monocyte adhesion to endothelial cells even in the presence of IL-1β. In light of these results, further investigation of miR-1914–5p could lead to the development of novel therapeutic strategies for atherosclerosis.

## CRediT authorship contribution statement

**Toshie Kihara:** Conceptualization, Methodology, Formal analysis, Investigation, Data curation, Writing – original draft, Visualization. **Kohki Toriuchi:** Conceptualization, Methodology, Formal analysis, Investigation, Data curation, Writing – original draft. **Hiromasa Aoki:** Conceptualization, Formal analysis, Writing – original draft. **Hiroki Kakita:** Conceptualization, Formal analysis, Writing – original draft, Funding acquisition. **Yasumasa Yamada:** Conceptualization, Formal analysis, Writing – review & editing, Funding acquisition. **Mineyoshi Aoyama:** Conceptualization, Formal analysis, Writing – review & editing, Supervision, Project administration, Funding acquisition, All authors read and approved the final manuscript.

## Declaration of competing interest

The authors declare that they have no known competing financial interests or personal relationships that could have appeared to influence the work reported in this paper.

## Acknowledgements

We acknowledge the assistance of the Research Equipment Sharing Center at Nagoya City University. This work was supported in part by Grants-in-Aid for Scientific Research from the Japan Society for the Promotion of Science, KAKEN grant numbers 16K10101, 17K10197, 18K07832, and 20K08211.

## Appendix A. Supplementary data

Supplementary data to this article can be found online at https://doi.org/10.1016/j.bbrep.2021.101046.

## References

[1] G.K. Hansson, A.K.L. Robertson, C. Söderberg-Nauclér, Inflammation and atherosclerosis, Annu. Rev. Pathol. 1 (2006) 297–329.
[2] G.R. Geovanini, P. Libby, Atherosclerosis and inflammation: overview and updates, Clin. Sci. 132 (2018) 1243–1252.
[3] R. Ross, Atherosclerosis — an inflammatory disease, N. Engl. J. Med. 340 (1999) 115–126.
[4] Y.V. Bobryshev, Monocyte recruitment and foam cell formation in atherosclerosis, Micron 37 (2006) 208–222.
[5] A.C. Li, C.K. Glass, The macrophage foam cell as a target for therapeutic intervention, Nat. Med. 8 (2002) 1235–1242.
[6] T. Waehre, A. Yndestad, C. Smith, T. Haug, S.H. Tunheim, L. Gullestad, S. S. Frøland, A.G. Semb, P. Aukrust, J.K. Damås, Increased expression of interleukin-1 in coronary artery disease with downregulatory effects of HMG-CoA reductase inhibitors, Circulation 109 (2004) 1966–1972.
[7] C.A. Dinarello, Proinflammatory cytokines, Chest 118 (2000) 503–508.
[8] V. Makó, J. Czúcz, Z. Weiszhár, E. Herczenik, J. Matkó, Z. Prohászka, L. Cervenak, Proinflammatory activation pattern of human umbilical vein endothelial cells induced by IL-1β, TNF-α, and LPS, Cytometry 77 (2010) 962–970.
[9] J. H Von Thusen, J. Kuiper, T.J.C. Van Berkel, E.A.L. Biessen, Interleukins in atherosclerosis: molecular pathways, Pharmacol. Rev. 55 (2003) 133–166.
[10] X. Wang, G.Z. Feuerstein, J.L. Gu, P.G. Lysko, T.L. Yue, Interleukin-1β induces expression of adhesion molecules in human vascular smooth muscle cells and enhances adhesion of leukocytes to smooth muscle cells, Atherosclerosis 115 (1995) 89–98.
[11] S.J. Mancini, D. Boyd, O.J. Katwan, A. Strembitska, T.A. Almabrouk, S. Kennedy, T. M. Palmer, I.P. Salt, Canagliflozin inhibits interleukin-1β-stimulated cytokine and chemokine secretion in vascular endothelial cells by AMP-activated protein kinase-dependent and -independent mechanisms, Sci. Rep. 8 (2018) 1–14.
[12] A. Tenenbaum, E.Z. Fisman, Mirroring the CANTOS revolution: is anti-inflammatory therapy for diabetes just around the corner? Cardiovasc. Diabetol. 16 (2017) 4–6.
[13] Y. Lu, The impact of microRNA in atherosclerosis, Arterioscler. Thromb. Vasc. Biol. 38 (2019) e159–e170.
[14] J. Winter, S. Jung, S. Keller, R.I. Gregory, S. Diederichs, Many roads to maturity: MicroRNA biogenesis pathways and their regulation, Nat. Cell Biol. 11 (2009) 228–234.
[15] F. Pankratz, C. Hohnloser, X. Bemtgen, C. Jaenich, S. Kreuzaler, I. Hoefer, G. Pasterkamp, J. Mastroianni, R. Zeiser, C. Smolka, L. Schneider, J. Martin, M. Juschkat, T. Helbing, M. Moser, C. Bode, S. Grundmann, MicroRNA-100 suppresses chronic vascular inflammation by stimulation of endothelial autophagy, Circ. Res. 122 (2018) 417–432.
[16] C. Pérez-Sánchez, M.Á. Aguirre, P. Ruiz-Limón, M.C. Ábalos-Aguilera, Y. Jiménez-Gómez, I. Arias-De La Rosa, A. Rodriguez-Ariza, L. Fernández-Del Río, J. A. González-Reyes, P. Segui, E. Collantes-Estévez, N. Barbarroja, F. Velasco, S. Sciascia, I. Cecchi, M.J. Cuadrado, J.M. Villalba, C. López-Pedrera, Ubiquinol effects on antiphospholipid syndrome prothrombotic profile: a randomized, placebo-controlled trial, Arterioscler. Thromb. Vasc. Biol. 37 (2017) 1923–1932.
[17] T. Staszel, B. Zapała, A. Polus, A. Sadakierska-Chudy, B. Kieć-Wilk, E. Stępień, I. Wybrańska, M. Chojnacka, A. Dembińska-Kieć, A Role of microRNAs in endothelial cell pathophysiology, Pol. Arch. Med. Wewn. 121 (2011) 361–367.
[18] J.L. Marques-Rocha, M. Samblas, F.I. Milagro, J. Bressan, J.A. Martínez, A. Marti, Noncoding RNAs, cytokines, and inflammation-related diseases, Faseb. J. 29 (2015) 3595–3611.
[19] M. Ohta, T. Kihara, K. Toriuchi, H. Aoki, S. Iwaki, H. Kakita, Y. Yamada, M. Aoyama, IL-6 promotes cell adhesion in human endothelial cells via microRNA-126–3p suppression, Exp. Cell Res. 393 (2020) 112094.
[20] J.E. Freedman, B. Ercan, K.M. Morin, C.T. Liu, L. Tamer, L. Ayaz, M. Kanadasi, D. Cicek, A.I. Seyhan, R.E. Akilli, C. Camci, B. Cengiz, S. Oztuzcu, K. Tanriverdi, The distribution of circulating microRNA and their relation to coronary disease, F1000Research 1 (2012) 1–12.
[21] X. Wang, Improving microRNA target prediction by modeling with unambiguously identified microRNA-target pairs from CLIP-ligation studies, Bioinformatics 32 (2016) 1316–1322.
[22] N. Wong, X. Wang, miRDB: an online resource for microRNA target prediction and functional annotations, Nucleic Acids Res. 43 (2015) D146–D152.
[23] Y. Kanda, Investigation of the freely available easy-to-use software "EZR" for medical statistics, Bone Marrow Transplant. 48 (2013) 452–458.
[24] K.J. Moore, F.J. Sheedy, E.A. Fisher, Macrophages in atherosclerosis: a dynamic balance, Nat. Rev. Immunol. 13 (2013) 709–721.
[25] K. Kitagawa, M. Matsumoto, T. Sasaki, H. Hashimoto, K. Kuwabara, T. Ohtsuki, M. Hori, Involvement of ICAM-1 in the progression of atherosclerosis in APOE-knockout mice, Atherosclerosis 160 (2002) 305–310.
[26] J. Galea, J. Armstrong, P. Gadsdon, H. Holden, S.E. Francis, C.M. Holt, Interleukin-1β in coronary arteries of patients with ischemic heart disease, Arterioscler. Thromb. Vasc. Biol. 16 (1996) 1000–1006.
[27] C.A. Dinarello, Interleukin-1 in the pathogenesis and treatment of inflammatory diseases, Blood 117 (2011) 3720–3732.
[28] E.V. Kazakova, M. Chen, E. Jamaspishvili, Z. Lin, J. Yu, L. Sun, H. Qiao, Association between RBMS1 gene rs7593730 and BCAR1 gene rs7202877 and Type 2 diabetes mellitus in the Chinese Han population, Acta Biochim. Pol. 65 (2018) 377–382.
[29] K. Kamide, Y. Kokubo, J. Yang, T. Matayoshi, N. Inamoto, S. Takiuchi, T. Horio, Y. Miwa, M. Yoshii, H. Tomoike, C. Tanaka, M. Banno, T. Okuda, Y. Kawano, T. Miyata, Association of genetic polymorphisms of ACADSB and COMT with human hypertension, J. Hypertens. 25 (2007) 103–110.
[30] Y. Lai, X. Zhang, Z. Zhang, Y. Shu, X. Luo, Y. Yang, X. Wang, G. Yang, L. Li, Y. Feng, The microRNA-27a: ZBTB10-specificity protein pathway is involved in follicle stimulating hormone-induced VEGF, Cox2 and survivin expression in ovarian epithelial cancer cells, Int. J. Oncol. 42 (2013) 776–784.
[31] C. Lopez-Pedrera, N. Barbarroja, A.M. Patiño-Trives, M. Luque-Tévar, C. Torres-Granados, M.A. Aguirre-Zamorano, E. Collantes-Estevez, C. Pérez-Sánchez, Role of micrornas in the development of cardiovascular disease in systemic autoimmune disorders, Int. J. Mol. Sci. 21 (2020) 1–30.
[32] C.C. Scholz, M.A.S. Cavadas, M.M. Tambuwala, E. Hams, J. Rodríguez, A. Von Kriegsheim, P. Cotter, U. Bruning, P.G. Fallon, A. Cheong, E.P. Cummins, C. T. Taylor, Regulation of IL-1β-induced NF-κB by hydroxylases links key hypoxic

and inflammatory signaling pathways, Proc. Natl. Acad. Sci. U.S.A. 110 (2013) 18490–18495.
[33] L.Y. Chu, Y.C. Hsueh, H.L. Cheng, K.K. Wu, Cytokine-induced autophagy promotes long-term VCAM-1 but not ICAM-1 expression by degrading late-phase IκBα, Sci. Rep. 7 (2017) 1–13.
[34] X. Huang, Y. Li, X. Li, D. Fan, H.B. Xin, M. Fu, TRIM14 promotes endothelial activation via activating NF-κB signaling pathway, J. Mol. Cell Biol. 12 (2020) 176–189.
[35] X. Sun, R.M. Baron, M.W. Feinberg, X. Sun, B. Icli, A.K. Wara, N. Belkin, S. He, L. Kobzik, R.M. Baron, M.W. Feinberg, MicroRNA-181b regulates NF- k B – mediated vascular inflammation, J. Clin. Invest. 122 (2012) 1973–1990.
[36] B. Bai, Y. Yang, Q. Wang, et al., NLRP3 inflammasome in endothelial dysfunction, Cell Death Dis. 11 (9) (2020) 776.
[37] M. Oelze, S. Kröller-Schön, P. Welschof, et al., The sodium-glucose co-transporter 2 inhibitor empagliflozin improves diabetes-induced vascular dysfunction in the streptozotocin diabetes rat model by interfering with oxidative stress and glucotoxicity, PloS One 9 (11) (2014), e112394.
[38] M. Takahashi, U. Ikeda, J.I. Masnama, S.I. Kitagawa, T. Kasahara, M. Saito, S. Kano, K. Shimada, Involvement of adhesion molecules in human monocyte adhesion to and transmigration through endothelial cells in vitro, Atherosclerosis 108 (1994) 73–81.
[39] C.A. Dinarello, Immunological and inflammatory functions of the interleukin-1 family, Annu. Rev. Immunol. 27 (2009) 519–550.
[40] S. Liu, D. Qu, W. Li, et al., miR 647 and miR 1914 promote cancer progression equivalently by downregulating nuclear factor IX in colorectal cancer, Mol. Med. Rep. 16 (6) (2017) 8189–8199.